Computer Communications 222 (2024) 241–255

Contents lists available at ScienceDirect

Computer Communications

journal homepage: www.elsevier.com/locate/comcom

Analysis of mobility robustness optimization in ultra-dense heterogeneous networks

Waheeb Tashan [a,*], Ibraheem Shayea [b,**], Sultan Aldirmaz-Colak [c]

[a] Department of Electrical and Electronics Engineering, Istanbul Medipol University, 34810 Istanbul, Turkey
[b] Electronics and Communication Engineering Department, Faculty of Electrical and Electronics Engineering, Istanbul Technical University (ITU), 34467, Istanbul, Turkey
[c] Department of Electrical and Electronics Engineering Istanbul Medipol University Istanbul, 34810 Turkey

ARTICLE INFO

INDEX TERMS:
Heterogeneous networks
Handover
Handover margin
Mobility robustness optimization
Time-to-trigger

ABSTRACT

Stable and reliable wireless connections during the user equipment's mobility are the critical issue in future mobile communication networks especially during UE's high-speed scenarios over dense heterogeneous networks (HetNets). Thus, setting an accurate value for the handover control parameters (HCPs) (i.e., time-to-trigger (TTT) and handover margin (HOM)) at different speed scenarios is required for system performance. This study proposes six different systems and each one employs different HCP settings using various mobile speed scenarios over a HetNet. Several performance metrics (i.e., received signal reference power (RSRP), handover ping-pong (HOPP), radio link failure (RLF), handover probability (HOP), handover interruption time (HOIT), and handover failure (HOF)) were used as key performance indicators (KPIs) for systems evaluations. Furthermore, 20 users were evaluated in this study using a 40 ms measurement interval. The results show a different impacts of each system on the performance of the deployed HetNet. However, System 1 (lowest TTT & moderate HOM) was the best system in term of RSRP and RLF but on the expense of HOPP. Furthermore, assigning high level of the TTT and HOM (i.e., TTT >1000 ms and HOM >8 dB) leads to 0 HOPP but high RLFs. Moreover, the best system performance in term of HOP, HOIT, and HOF were System 6 (highest TTT & high HOM) with 0.06 %, 3 %, and 0.004 %, respectively. System 4 represents the best trading off system between HOPP and RLF due to the proper configuration of the HCPs. However, the aims of evaluating several systems based on fixed HCPs over several mobile speed scenarios were to see the behaviors of the systems performance when different setting values are applied. Furthermore, this study proposes a HO self-optimization algorithm for auto-tuning the HCPs. Weighted function algorithm along with a trigger timer is used for reducing unnecessary HOs while RLF minimized by setting a trigger timer under a certain conditions when the RSRP of the serving base station (BS) goes below the received signal strength indicators (RSSI). The proposed algorithm shows a significant improvement in term of HOPP, RLF, HOP, and HOF compared to System 4 and FLC algorithm. The RSRP of the proposed algorithm is kept within acceptable range. Thus, accurate setting values for the HCPs are significant to keep the tradeoff between RLF and HOPP at the minimum level.

1. Introduction

According to Ericsson mobility report released on June 2022, 4.4 billion fifth generation (5G) subscribers in 2027 are forecasted [1]. Consequently, the demand for high data rate will be increased. Hence, heterogeneous network (HetNet) has been proposed as a promising solution for providing high data rate demands. In contrast, ultra-dense HetNets with a massive connected devices creating serious mobility management issues due to the large number of handovers (HOs) and traffic loads. These issues such as radio link failure (RLF), handover failure (HOF), handover ping-pong (HOPP), and handover interruption time (HOIT) [2]. Moreover, sustaining the quality connection during high-speed scenarios still a critical challenge in mobility management since high-speed travelling trains and drones can creates a large frequent HOs.

Velocity aware in mobility robustness optimization (MRO) function

* Department of Electrical and Electronics Engineering, Istanbul Medipol University, 34810 Istanbul, Turkey
** Electronics and Communication Engineering Department, Faculty of Electrical and Electronics Engineering, Istanbul Technical University (ITU), 34467 Istanbul, Turkey
E-mail addresses: waheeb.tashan@medipol.edu.tr (W. Tashan), shayea@itu.edu.tr (I. Shayea).

https://doi.org/10.1016/j.comcom.2024.04.033
Received 4 February 2023; Received in revised form 22 February 2024; Accepted 24 April 2024
Available online 29 April 2024

was addressed in Refs. [3–11]. A statistical HO optimization algorithm over long-term evolution (LTE) environment was proposed using high-speed railway scenarios [3]. Moreover, the key performance indicators (KPIs) in Ref. [3] include received signal reference power (RSRP), received signal reference quality (RSRQ), and the rate of cell-resources-change. Therefore, a dynamic handover margin (HOM) should be applied to the algorithm for system accuracy since fixed configuration of the HCPs (i.e., time-to-trigger (TTT) and HOM) may lead to system degradation. In Ref. [4], the authors have proposed a frequent HO mitigation algorithm to lessen unwanted HOs for ultra-dense HetNets. Moreover, the algorithm determines whether the frequent HOs are related to fast-moving users or ping-pongs. In addition, the performance evaluation in Ref. [4] shows a significant improvement in throughputs and reduction in the overall HOs by 10.82 % and 79.56 %, respectively. However, the authors have not distinguished between real time traffic users, e.g., voice services and non-real time users who can tolerate some connection interruptions. A framework based on RSRP to reduce the probability of HOF and handover ping-pong (HOPP) was presented in Ref. [5]. Besides, the RSRP was evaluated to observe the behavior of the RSRP over a various speed scenarios (i.e., below 30 km/h) using inter HO in macro cell (MC) and femtocell environment [6]. has proposed a velocity-aware HO self-optimization algorithm based on user equipment's (UE) speed and RSRP to adapt HCPs in HetNet. In addition, the aim of this study is to reduce the handover probability (HOP), RLF, and HOPP of all measured UEs. The authors in Ref. [7] have proposed a HO optimization algorithm to minimize the rate of RLF and HOPP. Moreover, the study has placed a statistical threshold instead of using TTT. Furthermore, a chain structure of evolved node B (eNBs) has been used along railway to evaluate UE's speed scenarios (i.e., 120 km/h, 250 km/h, and 350 km/h). A HO approach to self-optimization the HOM and cell individual offset over several speed scenarios (i.e., up to 360 km/h) was addressed in Ref. [8]. Besides, RLF and HOIT were used in this study as KPIs. In additional, mobile relay-node-based was presented as a communication network structure in railway high-speed environment. Therefore, TTT should be investigated in Ref. [8] as an additional parameter since TTT is one of the most essential control parameters in HO. UE takes the RSRP measurements and the HO decision is applied according to these measurements. However, inaccurate setting of TTT affects on system performance. Assigning different HOM values based on speed scenarios have been introduced in Ref. [9] where the low HOM values were used in high-speed scenarios whereas high HOM values were assigned to low-speed scenarios. Furthermore, fixed TTT and HOM values were evaluated using the KPIs which include RSRP, HOP, HOPP, RLF, HOIT, and HOF [10]. In Ref. [11], signal-to-interference-plus-noise-ratio (SINR), HOPP, and RLF were used as the KPIs over 5G network to optimize the TTT and HOM. In addition, the evaluated algorithm in Ref. [12] shows 75 % reduction in HOPP compared to distance algorithm in Refs. [13–15], cost function in Ref. [16], and fuzzy logic controller (FLC) in Ref. [17].

Weighted function has been applied as a solution in various MRO studies as addressed in Ref. [18]. In addition,A new weight function is applied in Ref. [19] to self-optimize HOM based on three function, SINR, traffic load, and velocity. In addition, the proposed algorithm is applied carrier aggregation operation over LTE-advanced system in order to enhance the throughput and minimize the outage probability. Article [20] has proposed a self-optimization algorithm over 5G network. Moreover, RSRP, HOP, HPPP, RLF were used as a KPIs for auto-tuning the TTT and HOM based on three criteria (i.e., SINR, traffic load, and velocity).

Although several studies have investigated HCPs in MRO, further evaluations are still required to achieve optimal HCP settings that is capable for obtaining system stability and reliability. However, to maintain the quality connection during HOs, accurate settings of TTT and HOM are required. However, the optimal HCP settings become more critical when several mobile speed scenarios are applied at a HetNet environment.

In this study, six different systems with various settings of HCPs (i.e., TTT and HOM) over HetNets have been proposed. Furthermore, all these systems have been investigated with various mobile speed scenarios (i.e., up to 200 km/h) to show the performance of each system upon each speed scenario. The systems' performances have been presented using several KPIs such as RSRP, HOPP, RLF, HOP, HOIT, and HOF. Therefore, addressing different systems with different mobile speed scenarios over HetNets will highlight the effects of HCP settings on the system performance when the speed changes. This will subsequently open a gate for further investigations for researches to propose a proper HO self-optimization algorithm at different HCPs with several mobile speed scenarios. Moreover, this study proposes a HO self-optimization algorithm for auto-tuning the HCPs during the HO process. Weighted function algorithm along with a trigger timer is used for reducing unnecessary HOs while RLF minimized by setting a trigger timer under a certain conditions when the RSRP of the serving base station (BS) goes below the received signal strength indicators (RSSI).

The remainder of this paper is organized as follows: Section 2 presents the relevant studies. Section 3 discusses the system model. Section 4 provides the KPIs for system evaluations. Section 5 presents the results and discussions. Section 6 highlights the future directions. Finally, Section 7 concludes this paper.

2. Relevant studies

Various studies were presented with different system models, and different mobility as well as different KPIs. However, these studies either implemented using conventional programming techniques or artificial intelligent techniques. Therefore, these relevant studies have been extensively presented in our surveys [18,21].

2.1. Conventional programming techniques in MRO functions

Since the introducing of MRO in Rel.9 of the third-generation-partnership-project (3GPP), various algorithms with different accuracy level have been investigated. However, this subsection highlights a brief introduction about a conventional programming techniques used for optimizing the HCPs of the MRO function. These algorithms include RSRP-based [22–31], weight function [12], [19,20,32,33], FLC [17, 34–37], velocity-aware [3–8,38], UE speed with traffic load [17], dwelling time [39]. Furthermore, integrated techniques have been applied in MRO for optimal HCP settings such as fuzzy-analytic hierarchy process [40] and fuzzy with technique for order of preference by similarity to ideal solution [41].

The differences in the input, output parameters, KPIs, and fuzzy rules have led to variances in adjusting the HCPs setting value for each algorithm. For instance, RSRP, RSRQ, SINR, number of resource blocks, traffic load, and UE's speed are the common input parameters used for optimizing TTT and HOM.

2.2. Artificial intelligence in optimization algorithms

Due to the difficulties to deal with the optimization parameters by using a conventional interpolation techniques, machine learning optimizes the HCPs (i.e., TTT and HOM) through learning, automatic extraction of knowledge, mapping out the functions that cannot be interpreted mathematically, and choosing the optimal action based on the rewards achieved [42]. However, increasing the demands (i.e., high data rate and capacity) throughout the mobile network evolutions require providing a suitable service to satisfy the users. To cope up with these demands, unplanned small dense HetNets have been deployed. Which will subsequently in increase the HO complexity. Besides, manual optimizing of these HetNets will increase the operational costs for the network operators. Therefore, reducing network complexity as well as decreasing the operational cost are the most common motivations to use the artificial intelligence (AI) in mobility management filed. Nowadays, AI has been used as a solution method toward obtaining an optimal HO settings by self-optimizing the HCPs of the MRO function. Next section will address in details the ML techniques used in MRO functions.

Various studies have presented a machine learning (ML) as a solution methodology for self-optimizing HCPs in mobility robustness optimization (MRO) function such as supervised ML in Refs. [43–49], unsupervised ML in Ref. [50], and reinforcement learning in Refs. [51–61]. The objective of these

studies is to adapt an optimal settings of the HCPs for system enhancement and accuracy. All of the aforementioned studies have applied various KPIs, different deployment scenarios, and different HCPs. Hence, obviously the variations in system performance will be different as addressed in Refs. [18,21].

The applied supervised ML techniques are linear regression with genetic algorithm [44], deep neural network (i.e., rectified linear unit and SoftMax function) [48], and neural network multilayer perceptron [45,46]. While from unsupervised ML, K-means clustering technique has been used in Ref. [50]. In addition, several reinforcement learning techniques have been addressed in MRO for self-optimizing the HCPs such as Q-learning [42,54,55,61,62], fuzzy Q-learning [51–53,56], and AHP-TOPSIS with Q-learning [57]. Deep reinforcement learning has been considered as a significant solution method in achieving the optimal setting value for HOM and TTT in HetNets since there is no optimal MRO function available [63].

3. System model

Network deployment scenario, network parameters, system setting, and simulation processes over the proposed HetNet environment have been addressed in this section. We assumed that the propagation environment is urban areas, thus the path-loss (PL) is calculated according to urban area model.

3.1. Network deployment scenario

Switching the network resources of the UE from base station (BS) to another BS has been illustrated in Fig. 1. As seen from the figure, each cell is divided into three sectors. Each sector includes small cell (SC). SC's size is small compared to MCs. Moreover, SCs and MCs have variations in their radio access technology (RAT). Furthermore, Table 1 illustrates the HO scenarios where two types of HOs (i.e., vertical and horizontal HO) are addressed in our simulation environment. A HetNet has been considered in the simulation environment which consists of MCs and 5G SCs as shown in Fig. 1. In addition, UEs are moving in one fixed direction using 10 mobile speed scenarios. Furthermore, 20 km/h, 40 km/h, 60 km/h, 80 km/h, 100 km/h, 120 km/h, 140 km/h, 160 km/h, 180 km/h, 200 km/h were the applied mobile speed scenarios of the UEs. Therefore, the serving BS handing over the network resources to the target BS based on the UE's measurement reports which have been sent to the serving BS. Therefore, the HO is executed if the HO decision algorithm in Table 1 is satisfied.

Table 1
Types of HO based on Fig. 1.

HO No.	HO cell type	Type of HO	RAT
HO1	**Macro to same Macro:** HO from sector to another sector inside the same MC	Horizontal	No
HO2	**Macro to mmWave:** HO from MC's sector to mmWave BS (i.e., SC)	Vertical	Yes
HO3	**mmWave to Macro:** HO from MC's sector to mmWave BS (i.e., SC)	Vertical	Yes
HO4	**Macro to another Macro:** HO from sector to another sector that located in different BS	Horizontal	No

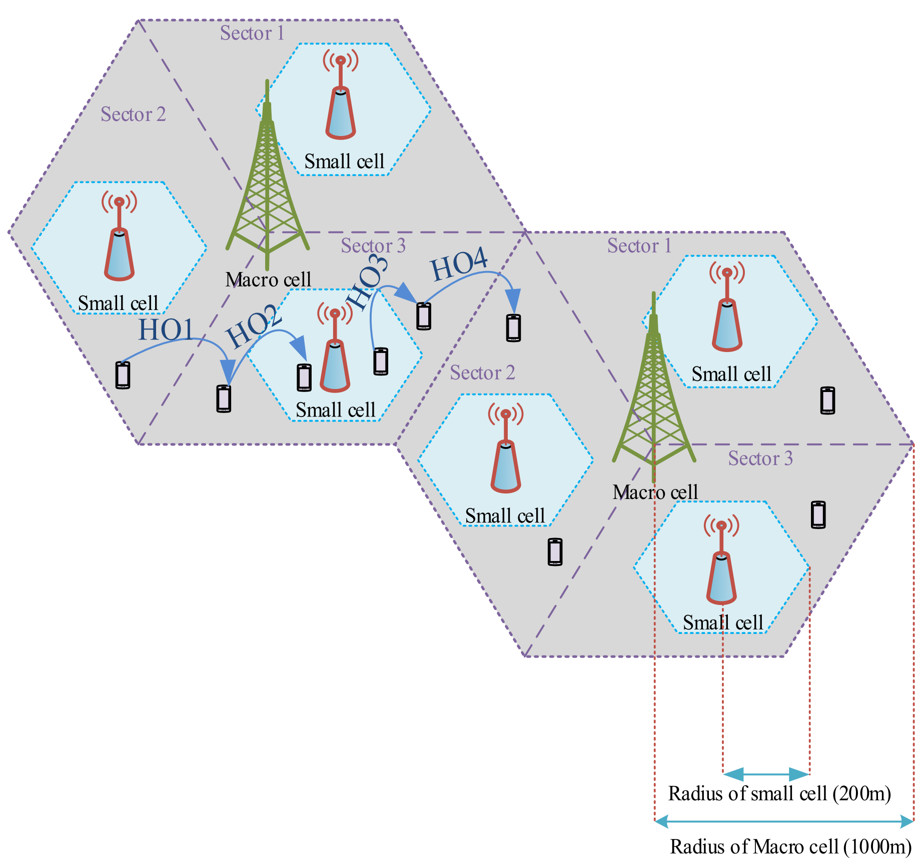

Fig. 1. System model for the HetNet.

Fig. 2 illustrates the deployed HetNet scenario in our study where three sectors in each MC were implemented and one SC is located in each sector, 61 MCs and 183 SCs. In additional, one re-use frequency is used in this study. Moreover, the SCs covers small geographical area due to their high frequency (i.e., 28 GHz) which the wavelength is narrow [64]. However, the simulation area covering 8×8 km^2 within an urban area.

3.2. Network parameters

Table 2 addresses the simulation parameters of our HetNet presented in Fig. 2. However, this study was simulated using MATLAB 2021b to examine the system performance by evaluating several settings of the HCPs over a HetNet. Moreover, the HCP setting values fall within the range assigned by 3GPP. However, two radio access technologies were supported in this work and allowing only one BS to be connected to the UE.

Moreover, 2.6 GHz and 28 GHz were the operating frequency applied to the macro BS and small BS, respectively. In addition, the minimum received power level is −101.5 dBm where the system may experience a RLF below this threshold [65]. However, the HO procedure (i.e., HO preparation, HO execution, and HO completion) is initiated as long as the HO decision algorithm in (1) satisfies. Furthermore, the assumptions of the simulation parameters addressed in Table 2 are based on 3GPP [6, 20,22,65,66].

3.3. Systems setting and simulation processes

Table 3 shows various HCP settings for the considered systems. Each system performance is evaluated at various mobile speed scenarios. However, controlling the HCPs during mobile speed scenarios has a great impact on system performance. For instance, high-speed case requires low TTT value to avoid late HOs whereas low speeds case requires high TTT value to avoid early HOs. Hence, HOPP.

probabilities and RLFs should be reduced due to assigning proper values for the HCPs. Fig. 3 addresses the simulation flowchart for the HetNet. However, it starts with identifying the network parameters, then building the HetNet environment followed by the mobility model of the simulated environment. Besides, in each simulation cycle (i.e., 40 ms), the direction and the position of each user is updated. Furthermore, the Euclidean distance from the BSs of each user at each simulation cycle is calculated. Moreover, the evolutions of the PL are estimated according to the calculated distances with the addition to log-normal shadowing. In addition, the flowchart includes the HO decision algorithm with trigger timer, which was explained in Fig. 4. The parameters T and T_{max}

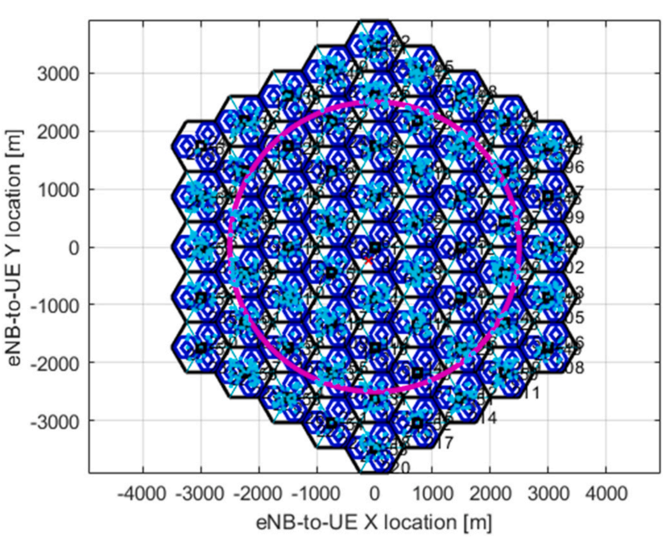

Fig. 2. Simulation environment for the HetNet.

Table 2
Simulation parameters.

Network Parameter	Assumption	
	Macro Cell	5G small cell
Cell radius (meter)	500	200
Number of BSs	61	183
Operating Frequency (GHZ)	2.6	28
BS transmitter Power (dBm)	46	30
BS height (meter)	25	15
Bandwidth (MHz)	20	500
UE max Tx power (dBm)	21	
UE min Tx power (dBm)	−50	
Q_rxlevmin[a](dBm)	−101.50	
UE height (meter)	1.5	
UE noise figure (dB)	9	
HOM (dB)	(2, 5, 8, 10)	
TTT (ms)	(320, 512, 1500, 2560, 4800)	
UE speeds (km/hr)	[20, 40, 60, 80, 100, 120, 140, 160, 180, 200]	
Number of measured UEs	20	
Measurement interval	40 ms	
HO decision algorithm	$RSRP_{Target} \geq RSRP_{Serving} + HOM$ (1)	
Environment	Urban areas, HetNet	

[a] Q_rxlevmin is the minimum received power level in dBm.

Table 3
Setting of HCPs in terms of TTT and HOM values.

System NO.	TTT(ms)	HOM(dB)
System 1	320	5
System 2	320	8
System 3	512	2
System 4	1500	8
System 5	2560	10
System 6	4800	8

stated in the flowchart represent the simulation cycle and the maximum number of simulation cycle, respectively. Moreover, the HO decision algorithm is satisfied when $RSRP_{Target} \geq RSRP_{Serving} + HOM$ at TTT interval. In addition, a procedure of HO self-optimization has been explained in our previous work [18].

3.4. Self-optimized handover control parameter algorithm

In this subsection, an automatic optimization of the HCPs (i.e., TTT and HOM) were applied using weighted function (WF) algorithm. In addition, a counter timer was addressed to reduce the unnecessary HOs as shown in Fig. 4. In contrast, the counter timer may increase the number of RLF of the system. However, we have excluded a timer counter shown in (7) when the serving BS below the received signal strength indicators (RSSI) in order to make a quick HO for RLFs reduction. Therefore, Algorithm 1 shows the instruction steps for the self-optimization process over a HetNet environment shown in Fig. 2 using Table 2 as a simulation parameters. Besides, types of HOs shown in Table 1 is used in this HO self-optimization process. Therefore, we have developed our weighted function in Ref. [19] since a partial optimization (i.e., HOM) was applied. In this work, TTT and HOM were optimized based on three input metrics (i.e., RSRP, UE's speed, and traffic load).

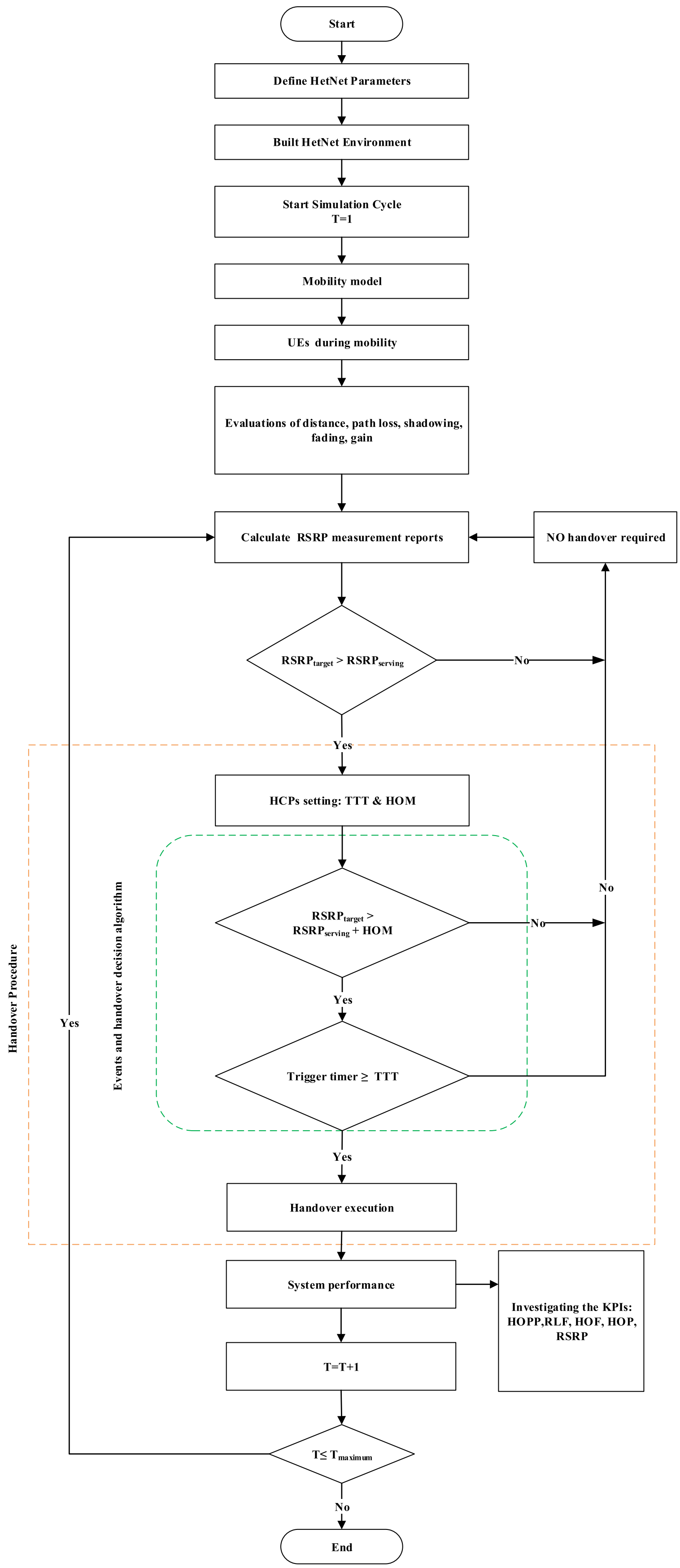

Fig. 3. Simulation flowchart for HO optimization in future HetNet.

Algorithm 1
Weighted function algorithm.

```
Algorithm 1 Weighted Function Algorithm
Start
Initialize HetNet parameters and mobility model
Initialize simulation cycles
Inputs: RSRP_serving, RSRP_target, UE's speed, traffic load
Output: HOM, TTT
Calculate the input parameters
if RSRP_target> RSRP_serving
Initialize WF
Update TTT and HOM according to (14)
Auto-tunes TTT and HOM
if T=1 then
HO decision ←— false
if RSRP_target> RSRP_serving+ HOM then
if trigger timer>= TTT then
HO decision ←— true
Send HO request
Initialize preparation, execution, and completion HO
if RSRP_serving < RSSI
No trigger timer is initiated
HO decision ←— true
Send HO request
Initialize preparation, execution, and completion HO
else HO decision ←— false
end if
```

4. Key performance indicators

To measure the HO performance of the network, well-known KPI set is used in the literature. In this study we present our simulation results in terms of RSRP, HOPP, RLF, HOP, handover interruption time (HOIT), and HOF.

When one of the HCP settings is changed or simultaneously change, a few of KPIs may increase and the others may decrease. Thus, we seek the optimal HCP setting which provides the acceptable KPIs values.

- **RSRP:** Two different models have been applied to measure the RSRP for the 5G HetNet. (2) and (3) represents the RSRP calculation of the MCs and the SCs, respectively. All RSRP and PL formulations are based on 3GPP release-16 [65]. RSRP basically depends on distance between the BS and the UE, antennas gain. The RSRP has been measured for each BS at each simulation cycle, for each measured user, and in each speed scenario.

$$RSRP(dBm) = PTx_{mac}(dBm) + G\ (dB) + G_{UE(dB)} - PL_{\ mac} + fading_{mac}, \tag{2}$$

where PTx_{mac} is the transmission power of the MC, G (dB) is the directional antenna gain applied, $G_{UE(dB)}$ is the gain for the user, $PL_{\ mac}$ is the path-loss for the MCs, $fading_{mac}$ is the MC fading.

$$RSRP(dBm) = PTx_{sm}(dBm) + G\ (dB) + G_{UE(dB)} - PL_{\ sm} + fading_{sm}, \tag{3}$$

where PTx_{sm} the transmission power of the SCs, G (dB) is the directional antenna gain applied, $G_{UE(dB)}$ is the gain for the user, $PL_{\ sm}$ is the path loss for the SC, and $fading_{sm}$ is the SC fading.

$$PL_{dB} = 40 \times \left(1 - 4\left(10^{-3}\right)d_{hb}\right)\log_{10}(R) - 18 \times \log_{10}(d_{hb}) + 21 \times \log_{10}(f) + 80dB, \tag{4}$$

where R is UE-BS separation in km, f is the carrier frequency in MHz, and d_{hb} is the BS antenna height. However, the operating frequency and the BS antenna height have been mentioned in Table 2. Moreover, two different PL models have been applied in this study by changing the operation frequency and BS antenna height in (4). For example, f and d_{hb} values used for MC are different from those used for SC as addressed in Table 2. Furthermore, fading and log-normal shadowing have been employed for the outdoor areas for measuring the RSRP.

- **HOPP:** The process is considered as HOPP when the UE bouncing back to the previous serving BS in time that is shorter than the critical time interval which defined as 2 s. In other word, the UE initiates the HO from BS A to BS B and then making a HO back to BS A within a time less than 2 s. Equation (5) obtains the average HOPP in all simulation cycles.

$$\overline{HOPP} = \frac{N_{HOPP}}{N_{HO}} \tag{5}$$

where N_{HO} represents all requested HOs as shown in (6).

$$N_{HO} = NF + NS, \tag{6}$$

where NF and NS are the failure and successful HOs, respectively, during the entire simulation time.

In order to reduce the probability of HOPP, a trigger timer has been introduced. However, the trigger timer addressed in Fig. 4 is based on our system model presented in Fig. 1. The objective of the trigger timer is to avoid the HO process from sector to the same sector or from SC to the same SC. The counter timer will be initiated along with the HO decision algorithm stated in Table 2. In addition, the

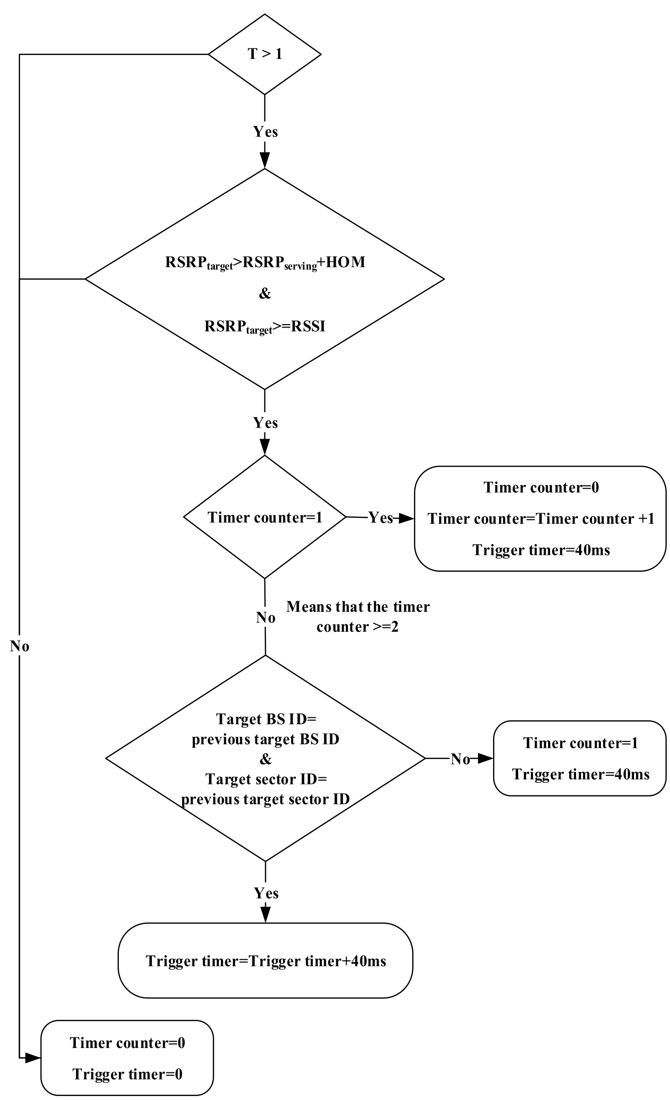

Fig. 4. Trigger timer for future mobile HetNet (T represents the simulation cycle).

maximum value for the timer counter for each user must satisfy (7):

$$Timer\ counter_{max=}\frac{TTT}{MI}. \tag{7}$$

Where MI is the measurement interval which equal to 40 ms. For example if TTT = 120 ms, the maximum timer counter has to be 120/40 = 3. This counter should count only if HO decision algorithm is satisfied and the target BS ID or sector ID has to be different from the previous simulation cycle. Otherwise, the counter timer will be set to zero. As shown in Fig. 4, the simulation cycle (T) starts from T > 1 since there is no HO triggering at T = 1.

- **RLF:** RLF occurs when $RSRP < RSSI$ where RSSI is the received signal strength indicator [23,67]. The following equation calculates the average probability of RLF ($\overline{RLF}$) for all simulation cycles for all UEs.

$$P(\overline{\mathrm{RLF}}) = \frac{\sum_{j=1}^{N_u} \mathrm{P(RLF)}}{\mathrm{N_u}}, \tag{8}$$

where N_u is the number of all measured users j in the simulation environment.

- **HOP:** HOP measures the HOs between the serving BSs and the target BSs. Hence, it is the probability of changing the radio resources between BSs. The average HOP for all users for all simulation cycles can be represented as:

$$\overline{HOP} = \sum_{j=1}^{N_u} \frac{HOP}{N_u}, \tag{9}$$

where $\mathrm{N_u}$ represents number of the measured users in the simulation environment.

- **HOIT:** The HO decision algorithm is used for HO triggering. Subsequently, the HO is performed to the BS that has the best measurement report. However, the HOIT occurs between HO command and HO completes [67]. HOIT is the time measured when there is not any exchange of user-plane packets with any of other BSs. Therefore, when the serving BS starts transmitting the HO command, the user-plane stops and the HOIT should be measured. The measurement ends as long as the HO is completed to the target BS. Therefore, HOIT is measured based on the 3GPP [67].
- **HOF:** HOF is one of the essential parameters for system performance. It can be calculated as a ratio of the number of unsuccessful HOs to the total number of HOs.

$$HOF = \frac{N_F}{N_F + N_S}, \tag{10}$$

where N_F and N_S are the number of failure HOs and the number of successful HOs, respectively.

5. Results and discussions

An appropriate setting of HCPs leads to the reduction of RLFs, HOPPs, and HOP which will subsequently enhance the network quality connections. However, this section discusses the simulation results of this work which is classified into two subsections as shown below.

5.1. Based on fixed handover control parameters

In this subsection, six different systems with fixed HCPs have been evaluated based on Table 3. Besides, each UE will be assigned to only one BS (i.e., either MC or SC). Furthermore, defining a minimum and a maximum HOM and TTT values are essential to guarantee that they are not out of the range. Moreover, the system performance is evaluated in terms of these KPIs: RSRP, HOPP, RLF, HOP, HOIT, and HOF.

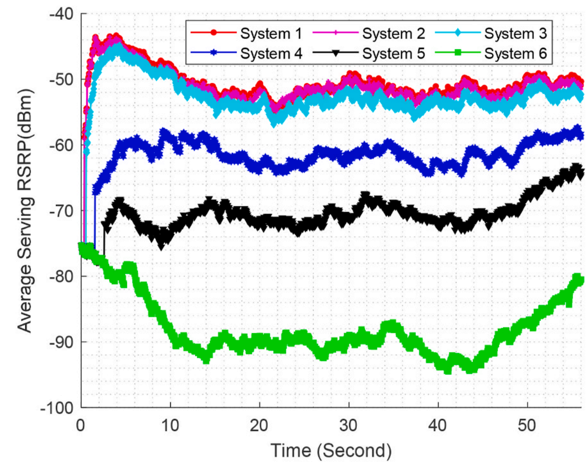

Fig. 5. Serving RSRP (dBm) for all users and all mobile speed scenarios vs simulation time.

5.1.1. Received signal reference power (RSRP)

The RSRP has been measured from all BSs periodically by the UE and the measurements have been reported to the serving BS. However, the HO will be triggered if all conditions have been met otherwise the UE is keeping the connection to the same serving BS, taking into account the measurement reports into consideration for triggering indication. However, HCPs (i.e., TTT and HOM) should be optimized properly based on the received signal level. For example, at high RSRP, low setting value should be set for the HCPs to keep the existing connection, while at low RSRP value, HCPs should have a low values to enable a smooth HOs [34]. Therefore, in this subsection, the RSRP simulated results of the six systems are discussed. The proposed systems parameters are given in Table 3. Six different TTT and five different HOM values are considered. According to this table, System 1 has the lowest TTT duration and this duration get higher as the system number increases. Frequent HOs usually occur in systems that has the lowest HOM and TTT value. In this paper we investigate which system outperforms all in terms of KPIs.

Fig. 5 shows the average serving RSRP (dBm) versus the whole simulation time. The systems presented in Fig. 5 have been evaluated by averaging all measured UEs and overall mobile speed scenarios. Furthermore, for each system, the RSRP was evaluated with different setting value of the TTT and HOM as mentioned in Table 3. However, setting high values for the HCPs as in System 6 leads to low RSRP values

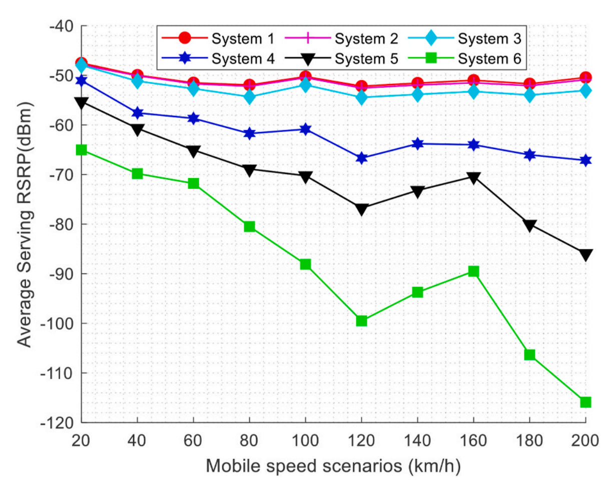

Fig. 6. Average RSRP at different mobile speed scenarios with six different systems.

while the RSRP values were strong in System 1 where low TTT and HOM are used overall simulation cycles (i.e., TTT = 320 ms, HOM = 5 dB). Since the TTT measurement interval and low HOM value, System 1 makes frequently HOs. Thus, the serving BS provides always a higher RSRP value for the UE in System 1. However, its signaling overhead is huge for the operator. As TTT or HOM value gets higher, the number of HOs gets low with high RLFs. These values are selected as the highest in System 6. Moreover, Fig. 5 shows very small differences in RSRP between System 1 and System 2 since they have a same TTT setting value with a small difference in their setting value of the HOM.

Fig. 6 represents the effects of HCPs setting value on RSRP in different mobile speed scenarios. It can be observed that increasing the setting value of the HCPs leads to decreasing the RSRP value. Actually, this figure can be interpreted in the same way as in Fig. 5. For high-speed scenarios, the signal power is faded quickly due to the path-loss. When the value of the TTT interval and/or HOM is high the transfer decision is made late. Therefore, the RSRP value continues to decrease. Moreover, in each system, the RSRP values were decreased when the user moves towards higher speeds. Therefore, it can be concluded that, high-speed scenarios require low TTT (ms) and low HOM (dB) for quick HO execution. In contrast, low speed case requires higher TTT and HOM values to keep the UE connect longer to the serving BS since the RSRP is strong. Furthermore, at low mobile speed scenarios (i.e., 20 km/h), the distance covered at a simulation time of 56 s is 0.311 km which means that the RSRP value is high in almost of the simulation cycles since the user slowly leaving the BS, while in high mobile speed scenario (i.e., 200 km/h), the user moves 3.11 km overall the simulation cycles. Based upon this, the RSRP values at low-speed scenarios are bigger than values in high-speed scenarios. Therefore, high mobile speed scenarios with high setting values of TTT and HOM may deteriorate the RSRP values as shown in System 6.

The RSRP values in Fig. 6 are averaged in order to obtain Fig. 7. Thus, the importance of fixed HCPs settings is highlighted. Each system has been evaluated individually in Fig. 7 to highlight the effect of the fixed HCPs settings. Fig. 7 represents the average RSRP over all mobile speed scenarios and all simulation time using all measured UEs.

As can be seen from the figure, Systems 1, 2, and 3 have similar RSRP values. System 1 and System 2 have the same TTT values and the HOM value of System 1 is 3 dB lower than that of System 2. Moreover, the TTT value of System 3 is 1.6 times greater than the TTT values of System 1 & 2 but its HOM margin is only 2 dB. Systems 4, 5, and 6 have higher TTT and HOM margin values, thus their number of handovers is lower than that of the previous Systems. Consequently, their serving RSRP values are small. In other words, using low setting values of TTT and HOM as in Systems 1, 2 and 3 has a small effect compared to using high setting value for the HCPs as in System 6. Besides, changing the value of TTT over the systems has a large effect on RSRP compared to HOM as in Systems 5 and 6.

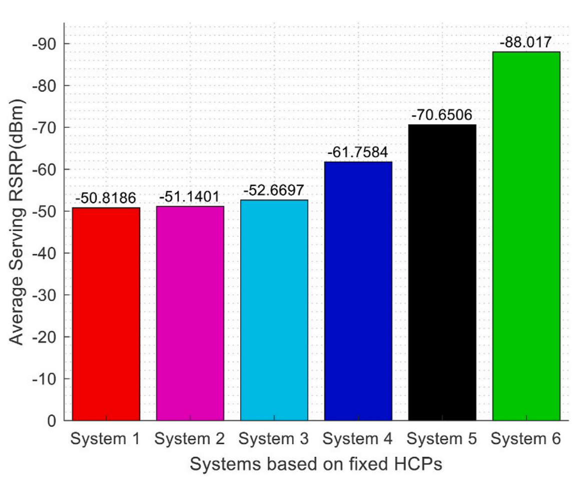

Fig. 7. Average serving RSRP vs fixed systems.

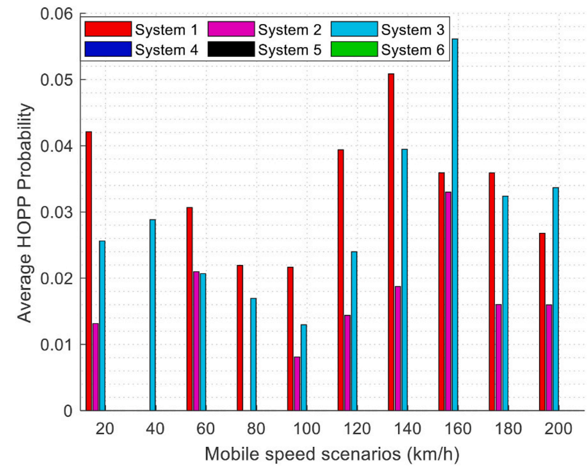

Fig. 8. Average HOPP probability at different mobile speed scenarios.

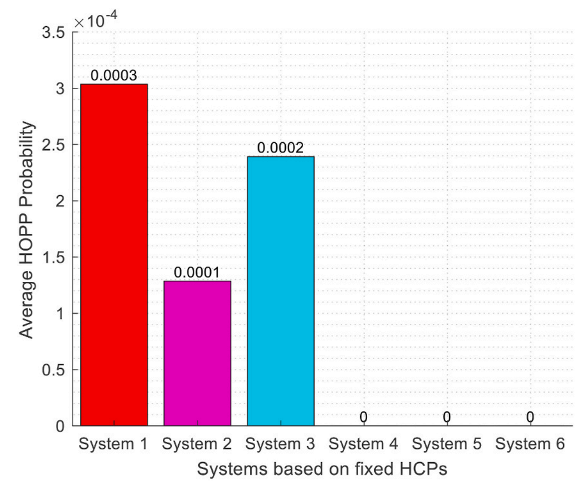

Fig. 9. Average HOPP Probability versus fixed systems.

5.1.2. *Handover ping-pong (HOPP)*

HOPP is one of the essential key performance indicators since minimizing the HOPPs may preserve the network resources and reduce the signaling overhead. However, HOPP may occur due to assigning a low setting value to the HCPs. Thereby, too early HOs may occur which leads to high HOPPs.

Fig. 8 represents the average HOPP probability at different mobile speed scenarios over all measured UEs and.

all simulation cycles. System 1 in Fig. 8 shows high HOPP due to low setting value of the HCPs except at 40 km/h where the HCP setting value was properly configured. Moreover, low value to the HOM was assigned to evaluate the behavior of System 3. It shows that the amount of HOPPs increasing proportionally with decreasing the setting values of TTT an HOM. In addition, no HOPPs occur in Systems 4, 5 and 6 due to very high setting value of the HCPs. Furthermore, 10 mobile speed scenarios were investigated in each system. However, the results indicates that, high mobile speed scenarios with high setting values of HCPs leads to RLF events rather than HOPPs which will be explained in RLF part.

Fig. 9 illustrates the average HOPP probability versus the fixed systems. However, assigning TTT and HOM that is greater than 1000 msec and 8 dB, respectively leads to zero HOPP. In addition, decreasing the HOM value may increase the HOPPs as shown in System 3 in Fig. 9. In

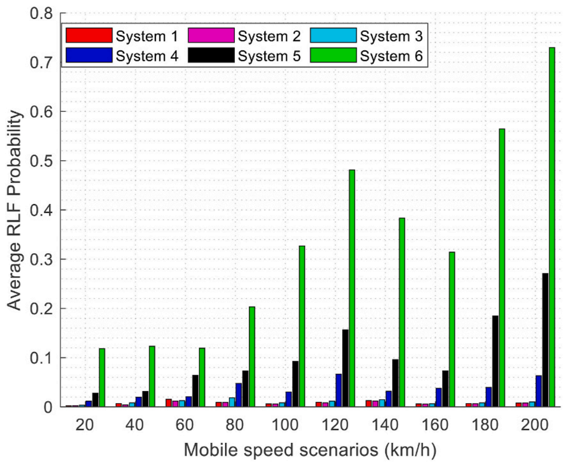

Fig. 10. Average RLF Probability versus different mobile speed scenarios.

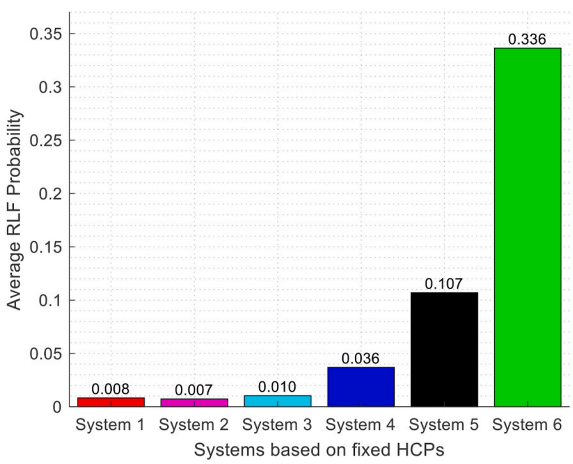

Fig. 11. Average RLF probability versus fixed systems.

summary, decreasing the setting values of the HCPs increases the occurrence of HOPPs while high HCPs may lead to low HOPPs but with high RLFs. Since System 1 and System 2 decide to handover according to the sudden fluctuation in signal level, their HOPP value is higher. However, since the TTT period is long in Systems 4, 5 and 6, it is decided to make a handover by observing for a longer period of time. For this reason, the decision is taken based on the change of location, not as a result of sudden changes. This reduces the HOPP value.

5.1.3. Radio link failure (RLF)

Fig. 10 represents the average RLF probability using 10 mobile speed scenarios over all measured UEs and all simulation cycles. It can be observed from Fig. 10 that System 6 represents the highest RLFs due to high setting value of the HCPs. In contrast to the HOPP events, RLFs occurs due to assigning high value to the TTT and HOM, especially for users that is in high-speed events or located at the cell edge. However, RLF should be reduced to enhance the system performance and enhance the network resources.

Fig. 11 highlights the average RLF probability for six systems at all simulation cycles and all mobile speed.

scenarios as well as for all measured UEs in order to evaluate the RLF events in each system. However, Systems 1, 2 and 3 show low HOFs since the setting values for the HCPs were not high compare to Systems 4, 5, and 6. Since the setting value of the HOM in System 2 was increased from 5 dB to 8 dB, a very small decreased in RLFs which means that it a proper setting value compare to System 1.

Table 4
Successful Handovers for each system over all measured UEs at 200 km/h.

System NO.	UE1	UE2	UE3	UE4	UE5	UE6	UE7	UE8	UE9	UE10	UE11	UE12	UE13	UE14	UE15	UE16	UE17	UE18	UE19	UE20
System 1	14	17	12	11	14	17	14	15	12	17	15	15	16	13	17	13	15	15	17	17
System 2	11	17	12	11	13	16	12	15	12	14	15	14	13	13	16	12	15	14	15	16
System 3	14	14	14	11	14	14	13	12	13	11	9	16	14	13	14	14	12	11	17	15
System 4	5	4	5	5	5	4	3	5	5	3	5	5	6	5	4	6	3	5	3	5
System 5	1	2	4	3	3	3	1	2	3	1	3	3	3	0	1	2	3	2	2	2
System 6	1	0	1	1	1	1	0	0	1	1	1	1	1	0	0	1	1	1	0	0

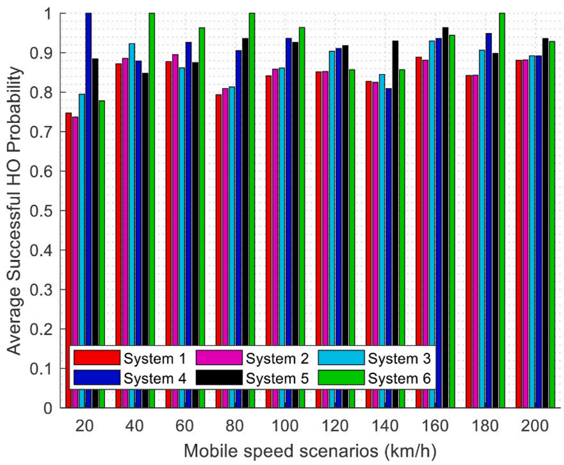

Fig. 12. Successful handover probability at different speed scenarios.

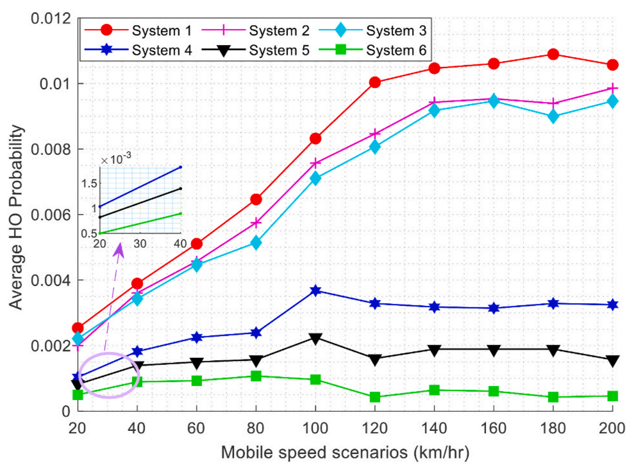

Fig. 13. Average Handover Probability at different speed scenarios.

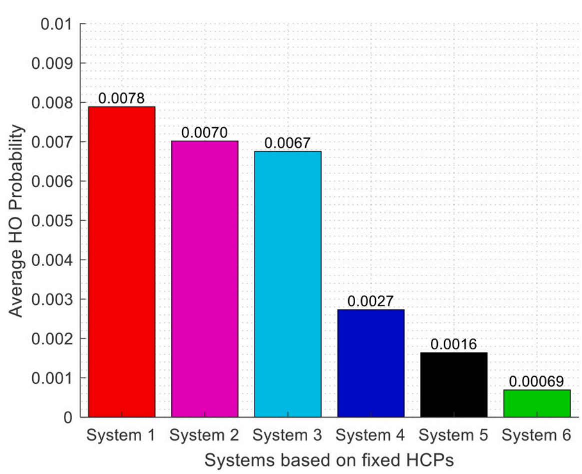

Fig. 14. Average Handover probability vs fixed systems.

5.1.4. *Handover probability (HOP)*

Before introducing the HO probability of all systems, the number of successful HOs for each UE at speed of 200 km/h will be highlighted in Table 4. Moreover, it can seen from the table that the number of the successful HOs decreases for each user when applying a high setting value for the TTT and HOM. This is because RLFs increases during high setting values whereas HOPPs increases during low setting values. The successful HOs can be measured by the number of the successful HOs to the total number of the requested HOs as shown in Fig. 12. In addition, Fig. 12 indicates to HOPPs when the successful HOs is not equal to the requested HOs (not equal to 1).

Fig. 13 shows the average HOP versus different mobile speed scenarios over all measured UEs and over all simulation cycles. However, as long as the system experiences low number of HOs, the system becomes more robust since unnecessary HOs will be reduced. However, HOP increases proportionally with the amount of HOPPs. Therefore, System 1 and System 6 in Fig. 13 have the greatest and the lowest HOPP, respectively. This will subsequently effect on the number of HOP as shown in Figs. 13 and 14. In addition, high HOPP leads to higher HOP which will subsequently effect on system performance. Therefore, the HOP was low when low speed scenarios were applied.

Fig. 14 evaluates the average HOP over all mobile speed scenarios, over all simulation cycles, and all measured UEs. Therefore, System 6 shows the lowest HOP because the system experience high RLF as shown in Fig. 11. Furthermore, the number of HOP and RLFs are inversely proportional to each other as shown in Figs. 14 and 11.

5.1.5. *Handover interruption time (HOIT)*

The average HOIT over all mobile speed scenarios and over all measured UEs are shown in Fig. 15. However, System 1 shows the highest interruption time among all 6 systems. Moreover, the HOIT at high-speed scenarios is higher compared to low-speed scenarios due to the high number of HO executions in high-speed scenarios since the UE moves longer distance.

Fig. 16 shows the HOIT over all simulation time, over all mobile speed scenarios, and all measured UEs. The figure evaluates the HOIT for each system. Therefore, System 1 shows the highest HOIT since it has a direct relation to HOP. In addition, as long as the HOP increases, the HOIT becomes worse.

5.1.6. *Handover failure (HOF)*

The average HOF probability versus six systems based on fixed HCPs are presented in Fig. 17. Besides, the HOF probability was implemented over all mobile speed scenarios, overall simulation cycles, and all measured UEs. However, System 1 was the worst system among other systems since the configuration of the HCPs were not suitable. In addition, System 1 creates the highest HOPPs compare to the other 5 systems which will subsequently increases the probability of HOFs. Moreover, System 6 was the best system since it shows the lowest average of the HOF probability. In contrast, it shows the highest RLFs as shown in Fig. 11. In summary, the setting value of the HCPs of each system may cause high HOPPs which leads to high HOP. Hence, the probability of

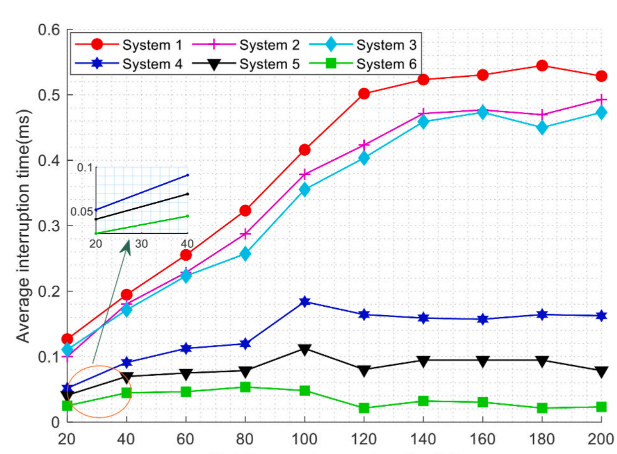

Fig. 15. Average HO interruption time for all UEs with different mobile.

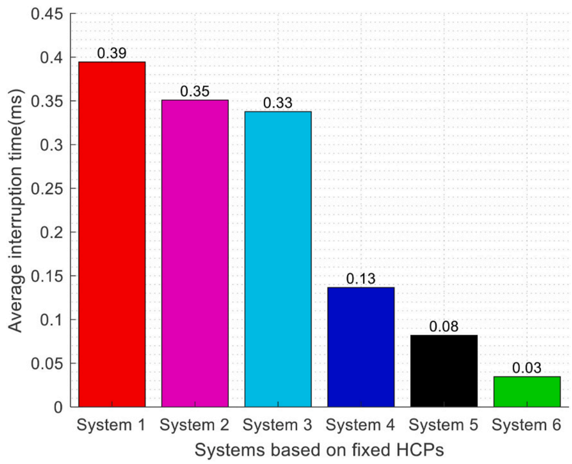

Fig. 16. Average HO interruption time vs fixed systems.

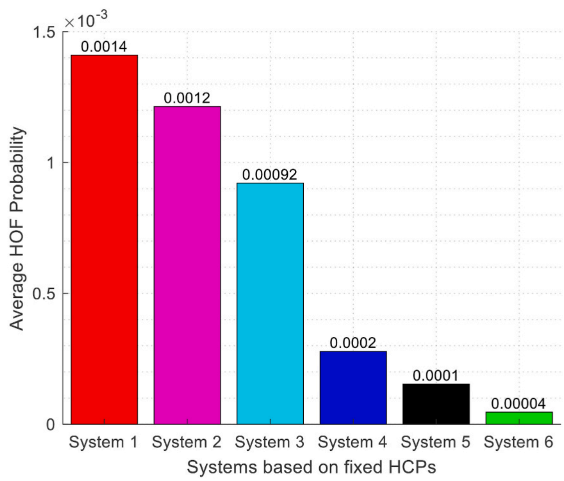

Fig. 17. Average HOF probability vs fixed systems.

getting high HOFs and HOIT is high. On the other side, setting fixed values may create a large amount of RLFs since the UE's received power level is below the threshold. Table 5 represents the performance of six systems when applying different HCPs. It can be seen that System1 shows the best RSRP compared to other systems while System 6 performs the best HOPP, HOP, HOIT, and HOF. In contrast, System 6 was the worst system in terms of HOFs since the configuration of HCPs were high (i.e., TTT = 4800 msec and HOM = 8 dB).

Table 6 shows the performance gain of the systems compared to the best reference system. For example, the RSRP for System 1 shown in Table 6 was considered the reference since it is the best RSRP among all applied systems. Hence, all other systems were compared to System1 in terms of RSRP to address the performance gain of other systems. Moreover, System 6 was the reference in term of HOP, HOIT, and HOF since it shows the lowest values compared to other systems.

In Table 7, the increment and decrement in KPIs are indicated by the up arrow and down arrow symbols, respectively. However, Table 7 evaluates the KPIs based on changing the TTT, HOM, and mobile speed scenarios. However, assigning low values to HCPs with increasing/or decreasing the mobile speed scenarios have a direct impact on KPIs which will subsequently effect on system performance. For example, System 1 was assigned with low value to the HCPs (i.e., TTT and HOM). So, when we apply a low mobile speed scenario to this system, the KPIs. Table 8 represents the list of abbreviations in alphapitical ordere.

will be affected as shown in Table 7. Moreover, when the setting value of the HCPs is high and the mobile speed scenario is decreased, the RSRP will be increased compared to high-speed scenarios with keeping the same setting value of the HCPs. Besides, assigning high TTT and HOM (i.e., HOM >8 dB), the HOPP will be decreased to 0 and the RLF will be increased. However, decreasing the HOM to 2 dB as shown in System 3 of Table 7 leads to increasing of the HOPP due to inappropriate configuration of the HCPs.

5.2. *Based on self-optimizing handover control parameters*

The simulation results have been enhanced based on algorithm 1 where self-optimization of the HCPs are applied. However, a tradeoff between HOPP and RLF was presented as shown in the previous subsection where a fixed setting value for the HCPs was applied. Therefore, System 4 was the best system addressed in term of the HOPP and RLF as shown in Figs. 9 and 11. However, this system is compared with the proposed WF algorithm and FLC [17] to show the improvement of HOPP and RLF when auto-tuning of HCPs are applied. Fig. 18 shows the serving RSRP over all measured users and all mobile speed scenarios. Even though the RSRP of proposed algorithm shows less RSRP values compared to FLC and FLC.

algorithm, but the performance of the proposed algorithm shows a significant reduction in the other KPIs as will be seen later. The RSRP of the WF shows an acceptable range. In addition, Fig. 19 shows that no HOPPs recorded in both System 4 and the proposed WF while the HOPPs were recorded for the FLC algorithm. Moreover, the proposed WF in Fig. 20 shows more reduction in RLFs compared to System 4. However, high average HOPP probability of the FLC shown in Fig. 19 led to more reduction in the average RLF probability as shown in Fig. 20. Furthermore, the WF in Fig. 21 is the lowest average HOP compared to System 4 and FLC algorithm. However, the amount of HOP significantly increase if the amount of HOPPs increase as addressed in HOPP of the FLC

Table 6
Performance gain evaluation of the systems.

KPIs	System 1	System 2	System 3	System 4	System 5	System 6
RSRP (dBm) (%)	**100**	99.7	98.2	89.1	80.2	62.8
HOPP (%)	99.18	99.99	99.98	100	**100**	100
RLF (%)	99.91	**100**	99.7	97.13	90.03	67.13
HOP (%)	99.28	99.36	99.39	99.79	99.9	**100**
HOIT (%)	64	68	70	90	95	**100**
HOF (%)	99.86	99.88	99.91	99.98	99.99	**100**

Table 5
Evaluations of the systems performances based on several KPIs.

KPIs	System 1	System 2	System 3	System 4	System 5	System 6	Average
RSRP (dBm) (%)	**−50.8**	−51.1	−52.6	−61.7	−70.6	−88	−62.46
HOPP (%)	0.03	0.01	0.02	0	0	**0**	0.01
RLF (%)	0.82	**0.73**	1.03	3.6	10.7	33.6	8.4133
HOP (%)	0.78	0.70	0.67	0.27	0.16	**0.06**	0.44
HOIT (%)	39	35	33	13	8	**3**	21.833
HOF (%)	0.14	0.12	0.09	0.02	0.01	**0.004**	0.064

Table 7
Effect of manual setting value of HCPs during changing of mobile speed scenarios.

System No	HCPs TTT (msec)	HCPs HOM (dB)	UE Speed Scenario	RSRP	HOPP	RLF	HOP	HOIT	HOF
1	320	5	Decreasing	↑	↑	↓	↓	↓	↓
			Increasing	↓	↑	↓	↑	↑	↓
2	320	8	Decreasing	↑	↑	↓	↓	↓	↓
			Increasing	↓	↑	↓	↑	↑	↓
3	512	2	Decreasing	↑	↑	↓	↓	↓	↓
			Increasing	↓	↑	↓	↑	↑	↓
4	1500	8	Decreasing	↑	↓	↑	↓	↓	↑
			Increasing	↓	↓	↑	↑	↑	↑
5	2560	10	Decreasing	↑	↓	↑	↓	↓	↑
			Increasing	↓	↓	↑	↑	↑	↑
6	4800	8	Decreasing	↑	↓	↑	↑	↑	↑
			Increasing	↓	↓	↑	↓	↓	↑

Table 8
List of abbreviations in alphabetical order.

Item	Description
3GPP	Third-generation partnership project
5G	Fifth generation
BS	Base station
eNB	Evolved node B
FLC	Fuzzy logic controller
HCP	Handover control parameters
HetNet	Heterogeneous networks
HO	Handover
HOF	Handover failure
HOIT	Handover interruption time
HOM	Handover margin
HOP	Handover probability
HOPP	Handover ping-pong
KPI	Key performance indicator
LTE	Long-term evolution
MC	Macro cells
ML	Machine learning
MRO	Mobility robustness optimization
PL	Path-loss (PL)
RAT	Radio access technology
RLF	Radio link failure
RSRP	Received signal reference power
RSRQ	Received signal reference quality
RSSI	Received signal strength indicators
SC	Small cell
SINR	Signal-to-interference-plus-noise-ratio
WF	Weighted function

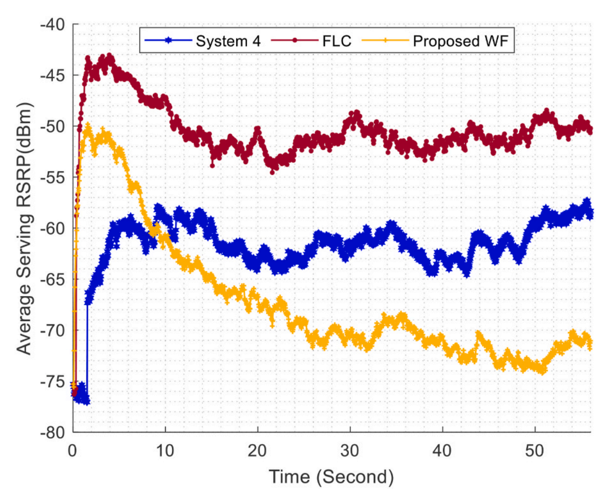

Fig. 18. Serving RSRP (dBm) for all users and all mobile speed scenarios vs simulation time.

algorithm. Furthermore, Fig. 22 represents the average HOP at different mobile speed scenarios over all measured UEs and all simulation time. In addition, the proposed algorithm shows the lowest average of the HOP compared to System 4 and to the FLC. The high HOPPs occurrence in FLC led to high average HOP. Besides, the requested HOs occurred in System 4 was higher than the requested HOs in the proposed WF. The average HOF probability for the WF addressed in Fig. 23 represents the average HOF probability versus HO optimization algorithms. Besides, the HO optimization algorithms were simulated at all mobile speed

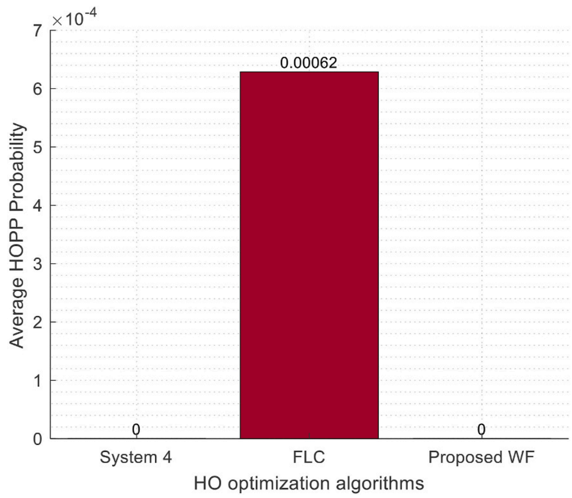

Fig. 19. Average HOPP Probability versus HO algorithms.

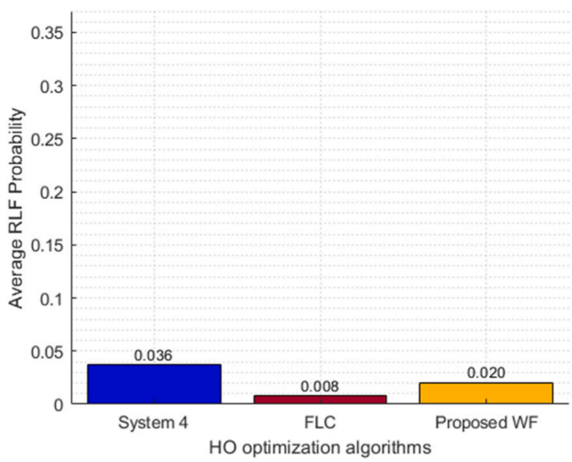

Fig. 20. Average RLF Probability versus HO algorithms.

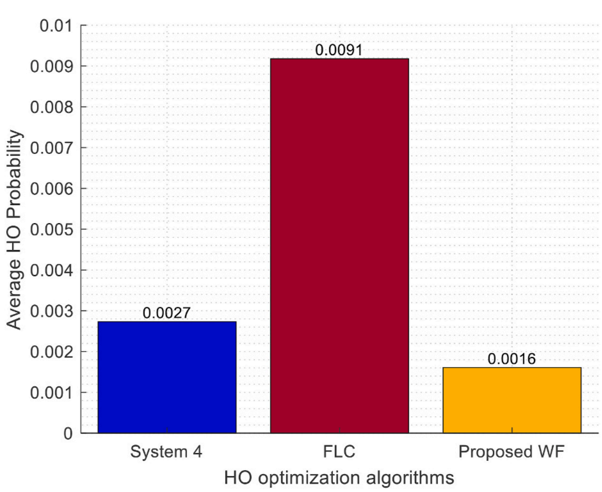

Fig. 21. Average Handover probability vs HO optimization algorithms.

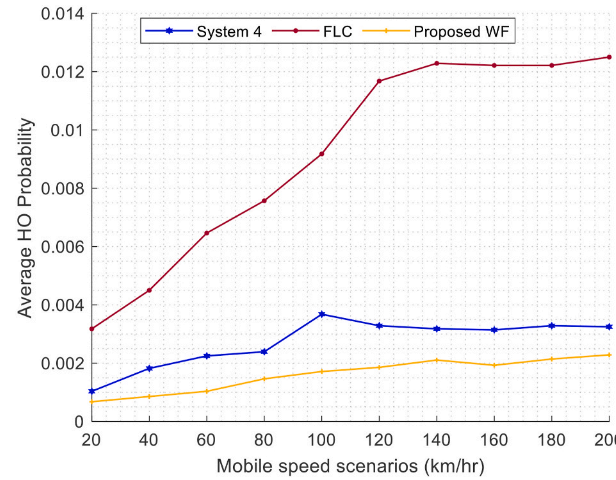

Fig. 22. Average Handover Probability at different speed scenarios.

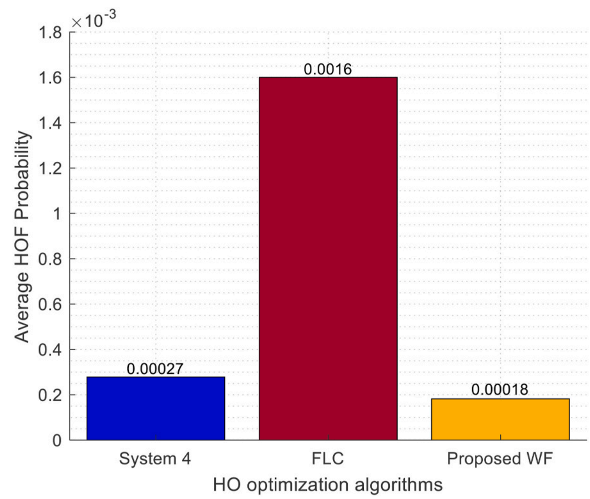

Fig. 23. Average HOF probability vs HO optimization algorithms.

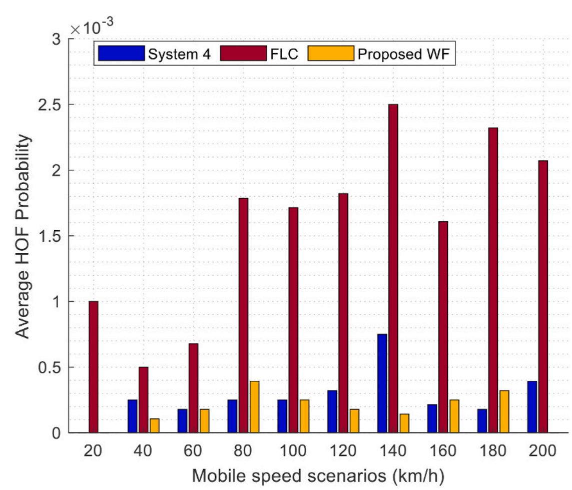

Fig. 24. Average HOF probability at different speed scenarios.

scenarios, over all measured UEs, and over all simulation time. In Fig. 24, the proposed WF has not recorded HOFs at speed scenarios of 20 km/h and 200 km/h while the average HOF probability at speed scenarios (i.e., 40 km/h, 120 km/h, 140 km/h) has recorded at lower level compared to System 4 and FLC.

6. Future directions

Up to date, a several proposed algorithms have been addressed in MRO function. These algorithms have been presented in section II. However, future work directions are addressed in this section to facilitate further research in this area.

- **Dual connectivity**

High mobile speed scenarios over an ultra-dense HetNet may create a large number of frequent HOs which will subsequently increase the ratio of HOPP and RLF. However dual connectivity may contribute to reduce these mobility issues (i.e., HOPP and RLF) in dense network deployments since the UE can connects to more than one target BS.

- **Deep reinforcement learning for MRO function**

Reinforcement learning specifically Q-learning needs instantaneous updates for every state-action pairs. This case is more complicated for future mobile networks and beyond where ultra-dense network are implemented. Consequently, large Q-table values are generated which become infeasible for maintaining. However, deep Q-learning superior capability compared to reinforcement learning in term of features extraction for predicting the optimized actions and rewards. In addition, deep reinforcement learning, which use deep Q-network, uses mini batches to store samples and the action state rewards which may accelerate the training process.

7. Conclusion

In this study, the systems performances of the fixed HCP values were evaluated and investigated. The cons of assigning a fixed value to the HCPs were comprehensively discussed. Furthermore, increasing the setting value of the HCPs results in decreasing the average HOPP probability and increasing in the average RLF probability. Moreover, the systems were evaluated over HetNet using several mobile speed scenarios. In addition, the system performance is evaluated by RSRP, HOPP, RLF, HOP, HOIT, and HOF. However, the simulation results illustrate that assigning high setting values to the HCPs may dramatically decease the HOPPs to 0 because of too late HOs which will cause a high RLFs especially at high-speed scenarios as shown in Fig. 10. In the other side, assigning low values to HCPs may reduce the RLF due to too early HOs but the HOPPs will be increased as shown in Fig. 8. However, the fixed systems were used as guidance on how to increase and decrease the HCPs in automatic way when several mobile speed scenarios are applied. Therefore, HO self-optimization algorithm is proposed and compared with other works. The simulation results demonstrated that the proposed algorithm shows improvement reduction in several KPIs (i.e., HOPP, RLF, HOP, and HOF).

CRediT authorship contribution statement

Waheeb Tashan: Conceptualization, Investigation, Methodology, Software, Writing – original draft. **Ibraheem Shayea:** Formal analysis, Project administration, Resources, Supervision, Validation. **Sultan Aldirmaz-Colak:** Supervision, Validation, Visualization, Writing – review & editing.

Declaration of competing interest

The authors declare that they have no known competing financial interests or personal relationships that could have appeared to influence the work reported in this paper.

Data availability

No data was used for the research described in the article.

Acknowledgment

This research study was supported by the Scientific and Technological Research Council of Turkey (TÜBİTAK) under Grant 118C276 conducted at Istanbul Technical University (ITU).

References

[1] Ericsson, Ericsson Mobility Report, June 2022.
[2] K. Kitagawa, T. Komine, T. Yamamoto, S. Konishi, A handover optimization algorithm with mobility robustness for LTE systems, in: 2011 IEEE 22nd International Symposium on Personal, Indoor and Mobile Radio Communications, 2011, pp. 1647–1651.
[3] F. Yang, H. Deng, F. Jiang, X. Deng, Handover optimization algorithm in LTE high-speed railway environment, Wireless Pers. Commun. 84 (2015/09/01 2015) 1577–1589.
[4] M.M. Hasan, S. Kwon, S. Oh, Frequent-handover mitigation in ultra-dense heterogeneous networks, IEEE Trans. Veh. Technol. 68 (2019) 1035–1040.
[5] M.S.N. Ali, A.L. Yusof, N. Ya'acob, M. Ismail, M.A. Zainali, M. Rosdi, et al., Handoff optimization in macrocell and femtocell LTE heterogeneous network, J. Telecommun. Electron. Comput. Eng. 9 (2017) 45–48.
[6] A. Alhammadi, M. Roslee, M.Y. Alias, I. Shayea, A. Alquhali, Velocity-aware handover self-optimization management for next Generation networks, Appl. Sci. 10 (2020) 1354.
[7] Y. Zhang, M. Wu, S. Ge, L. Luan, A. Zhang, Optimization of time-to-trigger parameter on handover performance in LTE high-speed railway networks, in: The 15th International Symposium on Wireless Personal Multimedia Communications, 2012, pp. 251–255.
[8] B. Davaasambuu, K. Yu, T. Sato, Self-optimization of handover parameters for long-term evolution with dual wireless mobile relay nodes, Future Internet 7 (2015) 196–213.
[9] Z. Wei, Mobility robustness optimization based on UE mobility for LTE system, in: 2010 International Conference on Wireless Communications & Signal Processing (WCSP), 2010, pp. 1–5.
[10] S. Alraih, R. Nordin, I. Shayea, N.F. Abdullah, A. Abu-Samah, A. Alhammadi, Effectiveness of handover control parameters on handover performance in 5G and beyond mobile networks, Wireless Commun. Mobile Comput. 2022 (2022).
[11] W.K. Saad, I. Shayea, B.J. Hamza, A. Azizan, M. Ergen, A. Alhammadi, Performance evaluation of mobility robustness optimization (MRO) in 5G network with various mobility speed scenarios, IEEE Access 10 (2022) 60955–60971.
[12] I.M. Bălan, B. Sas, T. Jansen, I. Moerman, K. Spaey, P. Demeester, An enhanced weighted performance-based handover parameter optimization algorithm for LTE networks, EURASIP J. Wirel. Commun. Netw. 2011 (2011) 1–11.
[13] 3GPP, Digital cellular telecommunications system (phase 2+); universal mobile telecommunications system (UMTS); LTE; telecommunication management; self-organizing networks (SON) policy network resource model (NRM) integration reference point (IRP); information service (IS), 3GPP TS 32.522 version 11.7.0 Release 11 (2013).
[14] 3GPP, "LTE; feasibility study for further advancements for E-UTRA (LTE-Advanced)", 3GPP (2018). TR 36.912 Version 15.0.0 Release 15 (2018) 3GPP.
[15] 3GPP, Telecommunication management; self-organizing networks (SON) policy network resource model (NRM) integration reference point (IRP); information service (IS), TS 28.627 version 15.0.0 Release 15 (2018).
[16] A. Miyim, M. Ismail, R. Nordin, Performance analysis of multi-level vertical handover in wireless heterogeneous networks, Wireless Pers. Commun. 95 (2017) 1109–1130.
[17] P. Muñoz, R. Barco, I.d. l. Bandera, On the potential of handover parameter optimization for self-organizing networks, IEEE Trans. Veh. Technol. 62 (2013) 1895–1905.
[18] W. Tashan, I. Shayea, S. Aldirmaz-Colak, M. Ergen, M.H. Azmi, A. Alhammadi, Mobility robustness optimization in future mobile heterogeneous networks: a survey, IEEE Access (2022) 1, 1.
[19] I. Shayea, M. Ismail, R. Nordin, M. Ergen, N. Ahmad, N.F. Abdullah, et al., New weight function for adapting handover margin level over contiguous carrier aggregation deployment scenarios in LTE-advanced system, Wireless Pers. Commun. 108 (2019) 1179–1199.
[20] I. Shayea, M. Ergen, A. Azizan, M. Ismail, Y.I. Daradkeh, Individualistic dynamic handover parameter self-optimization algorithm for 5G networks based on automatic weight function, IEEE Access 8 (2020) 214392–214412.

[21] W. Tashan, I. Shayea, S. Aldirmaz-Colak, O.A. Aziz, A. Alhammadi, Y. Daradkeh, Advanced mobility robustness optimization models in future mobile networks based on machine learning solutions, IEEE Access (2022) 1, 1.
[22] A. Alhammadi, M. Roslee, M.Y. Alias, I. Shayea, S. Alraih, K.S. Mohamed, Auto tuning self-optimization algorithm for mobility management in LTE-A and 5G HetNets, IEEE Access 8 (2020) 294–304.
[23] M.T. Nguyen, S. Kwon, H. Kim, Mobility robustness optimization for handover failure reduction in LTE small-cell networks, IEEE Trans. Veh. Technol. 67 (2018) 4672–4676.
[24] M.-h. Song, S.-H. Moon, S.-J. Han, Self-optimization of handover parameters for dynamic small-cell networks, Wireless Commun. Mobile Comput. 15 (2015) 1497–1517.
[25] A. Alhammadi, M. Roslee, M.Y. Alias, I. Shayea, S. Alraih, Dynamic handover control parameters for LTE-A/5G mobile communications, in: 2018 Advances in Wireless and Optical Communications (RTUWO), 2018, pp. 39–44.
[26] A. Abdulraqeb, R. Mardeni, A.M. Yusoff, S. Ibraheem, A. Saddam, Self-optimization of handover control parameters for mobility management in 4G/5G heterogeneous networks, Automat. Control Comput. Sci. 53 (2019) 441–451.
[27] A.A. Adewale, E. Ekong, F. Ibikunle, A. Orimogunje, J. Abolade, Ping-pong reduction for handover process using adaptive hysteresis margin: a methodological approach, IOP Conf. Ser. Mater. Sci. Eng. (2019) 012118.
[28] S. Zhang, G. Chuai, W. Gao, A handover optimization algorithm for LTE-R system handover parameter prediction and dynamic adjustment, in: International Conference in Communications, Signal Processing, and Systems, 2018, pp. 655–669.
[29] Y. Mal, J. Chen, H. Lin, Mobility robustness optimization based on radio link failure Prediction, in: 2018 Tenth International Conference on Ubiquitous and Future Networks (ICUFN), 2018, pp. 454–457.
[30] S. Chaudhuri, I. Baig, D. Das, Self organizing method for handover performance optimization in LTE-advanced network, Comput. Commun. 110 (2017) 151–163.
[31] M. Mehta, N. Akhtar, A. Karandikar, Impact of HandOver parameters on mobility performance in LTE HetNets, in: 2015 Twenty First National Conference on Communications (NCC), 2015, pp. 1–6.
[32] A. Alhammadi, W.H. Hassan, A.A. El-Saleh, I. Shayea, H. Mohamad, W.K. Saad, Intelligent coordinated self-optimizing handover scheme for 4G/5G heterogeneous networks, ICT Express 9 (2) (2022) 276–281.
[33] W. Zheng, H. Zhang, X. Chu, X. Wen, Mobility robustness optimization in self-organizing LTE femtocell networks, EURASIP J. Wirel. Commun. Netw. 2013 (2013/02/12 2013) 27.
[34] K.D.C. Silva, Z. Becvar, C.R.L. Frances, Adaptive hysteresis margin based on fuzzy logic for handover in mobile networks with dense small cells, IEEE Access 6 (2018) 17178–17189.
[35] A. Alhammadi, M. Roslee, M.Y. Alias, I. Shayea, S. Alriah, A.B. Abas, Advanced handover self-optimization approach for 4G/5G HetNets using weighted fuzzy logic control, in: 2019 15th International Conference on Telecommunications (ConTEL), 2019, pp. 1–6.
[36] V. Buenestado, J.M. Ruiz-Aviles, M. Toril, S. Luna-Ramirez, Mobility robustness optimization in enterprise LTE femtocells, in: 2013 IEEE 77th Vehicular Technology Conference (VTC Spring), 2013, pp. 1–5.
[37] K.C. Silva, Z. Becvar, E.H.S. Cardoso, C.R.L. Francês, Self-tuning handover algorithm based on fuzzy logic in mobile networks with dense small cells, in: 2018 IEEE Wireless Communications and Networking Conference (WCNC), 2018, pp. 1–6.
[38] S. Nie, D. Wu, M. Zhao, X. Gu, L. Zhang, L. Lu, An enhanced mobility state estimation based handover optimization algorithm in LTE-A self-organizing network, in: ANT/SEIT, 2015, pp. 270–277.
[39] S. Zang, W. Bao, P.L. Yeoh, H. Chen, Z. Lin, B. Vucetic, et al., Mobility handover optimization in millimeter wave heterogeneous networks, in: 2017 17th International Symposium on Communications and Information Technologies (ISCIT), 2017, pp. 1–6.
[40] R. Goyal, T. Goyal, S. Kaushal, H. Kumar, Fuzzy AHP based technique for handover optimization in heterogeneous network, in: Proceedings of 2nd International Conference on Communication, Computing and Networking, 2019, pp. 293–301.
[41] Y.S. Hussein, B.M. Ali, M.F.A. Rasid, A. Sali, A.M. Mansoor, A novel cell-selection optimization handover for long-term evolution (LTE) macro cell using fuzzy TOPSIS, Comput. Commun. 73 (2016) 22–33.
[42] M.T. Nguyen, S. Kwon, Machine learning–based mobility robustness optimization under dynamic cellular networks, IEEE Access 9 (2021) 77830–77844.
[43] B. Shubyn, T. Maksymyuk, Intelligent handover management in 5G mobile networks based on recurrent neural networks, in: 2019 3rd International Conference on Advanced Information and Communications Technologies (AICT), 2019, pp. 348–351.
[44] J. Shodamola, U. Masood, M. Manalastas, A. Imran, A machine learning based framework for KPI maximization in emerging networks using mobility parameters, 2020 IEEE international black sea conference on communications and networking, (BlackSeaCom) (2020) 1–6.
[45] P.-C. Lin, L.F.G. Casanova, B.K. Fatty, Data-driven handover optimization in next generation mobile communication networks, Mobile Inf. Syst. 2016 (2016) 1–11.
[46] S. Kumari, B. Singh, Data-driven handover optimization in small cell networks, Wireless Network 25 (2019/11/01 2019) 5001–5009.
[47] Z. Ali, M. Miozzo, L. Giupponi, P. Dini, S. Denic, S. Vassaki, Recurrent neural networks for handover management in next-generation self-organized networks, in: 2020 IEEE 31st Annual International Symposium on Personal, Indoor and Mobile Radio Communications, 2020, pp. 1–6.
[48] Z.H. Huang, Y.L. Hsu, P.K. Chang, M.J. Tsai, Efficient handover algorithm in 5G networks using deep learning, in: GLOBECOM 2020 - 2020 IEEE Global Communications Conference, 2020, pp. 1–6.
[49] B. Shubyn, N. Lutsiv, O. Syrotynskyi, R. Kolodii, Deep learning based adaptive handover optimization for ultra-dense 5G mobile networks, in: 2020 IEEE 15th International Conference on Advanced Trends in Radioelectronics, Telecommunications and Computer Engineering (TCSET), 2020, pp. 869–872.
[50] D. Castro-Hernandez, R. Paranjape, Optimization of handover parameters for LTE/LTE-A in-building systems, IEEE Trans. Veh. Technol. 67 (2018) 5260–5273.
[51] R.D. Hegazy, O.A. Nasr, H.A. Kamal, Optimization of user behavior based handover using fuzzy Q-learning for LTE networks, Wireless Network 24 (2018) 481–495.
[52] A. Klein, N.P. Kuruvatti, J. Schneider, H.D. Schotten, Fuzzy Q-learning for mobility robustness optimization in wireless networks, in: 2013 IEEE Globecom Workshops (GC Wkshps), 2013, pp. 76–81.
[53] J. Wu, J. Liu, Z. Huang, S. Zheng, Dynamic fuzzy Q-learning for handover parameters optimization in 5G multi-tier networks, in: 2015 International Conference on Wireless Communications & Signal Processing (WCSP), 2015, pp. 1–5.
[54] S.S. Mwanje, L.C. Schmelz, A. Mitschele-Thiel, Cognitive cellular networks: a Q-learning framework for self-organizing networks, IEEE Transactions on Network and Service Management 13 (2016) 85–98.
[55] A. Abdelmohsen, M. Abdelwahab, M. Adel, M.S. Darweesh, H. Mostafa, LTE handover parameters optimization using Q-learning technique, in: 2018 IEEE 61st International Midwest Symposium on Circuits and Systems (MWSCAS), 2018, pp. 194–197.
[56] P. Muñoz, R. Barco, I. de la Bandera, Load balancing and handover joint optimization in LTE networks using fuzzy logic and reinforcement learning, Comput. Network. 76 (2015) 112–125.
[57] T. Goyal, S. Kaushal, Handover optimization scheme for LTE-Advance networks based on AHP-TOPSIS and Q-learning, Comput. Commun. 133 (2019) 67–76.
[58] V. Yajnanarayana, H. Rydén, L. Hévizi, A. Jauhari, M. Cirkic, 5G Handover Using Reinforcement Learning, 2019 *arXiv preprint arXiv:1904.02572*.
[59] Q. Liu, C.F. Kwong, S. Wei, L. Li, S. Zhang, Intelligent handover triggering mechanism in 5G ultra-dense networks via clustering-based reinforcement learning, Mobile Network. Appl. (2021) 1–13.
[60] Q. Liu, C.F. Kwong, S. Wei, L. Li, Reinforcement Learning Based Joint Self-Optimisation Scheme for Fuzzy Logic Handover Algorithm in 5G HetNets, 2020 *arXiv preprint arXiv:2006.05010*.
[61] S. Shao, G. Liu, A. Khreishah, M. Ayyash, H. Elgala, T.D.C. Little, et al., Optimizing handover parameters by Q-learning for heterogeneous radio-optical networks, IEEE Photon. J. 12 (2020) 1–15.
[62] M.L. Marí-Altozano, S.S. Mwanje, S.L. Ramírez, M. Toril, H. Sanneck, C. Gijón, A service-centric Q-learning algorithm for mobility robustness optimization in LTE, IEEE Transactions on Network and Service Management 18 (2021) 3541–3555.
[63] W. Huang, M. Wu, Z. Yang, K. Sun, H. Zhang, A. Nallanathan, Self-Adapting handover parameters optimization for SDN-enabled UDN, IEEE Trans. Wireless Commun. (2022) 1, 1.
[64] W. Tashan, I. Shayea, S. Aldirmaz-Colak, T.A. Rahman, A.A. El-Saleh, M. Roslee, Rain rate and rain attenuation over millimeter waves in tropical regions based on real measurements, in: 2021 IEEE 15th Malaysia International Conference on Communication (MICC), 2021, pp. 120–125.
[65] 3GPP, LTE Evolved Universal Terrestrial Radio Access (E-UTRA) Radio Frequency (RF) System Scenarios, vol. 36, TR, 2020, p. 942, *version 16.0. 0 Release 16*.
[66] 3GPP, LTE; Evolved Universal Terrestrial Radio Access (E-UTRA); Base Station (BS) Radio Transmission and Reception, vol. 36, 3GPP TS, 2021, p. 104, *version 16.9.0 Release 16*.
[67] 3GPP, Evaluation Model for Rel-8 Mobility Performance, 2009, pp. R2–R92433.